

Clocking Convergence to Arnold Tongues - The H -rank Approach

Mantas Landauskas* and Minvydas Ragulskis

Center for Nonlinear Systems, Kaunas University of Technology, Studentu 50-147, Kaunas, LT-51368, Lithuania

Received: 2 Feb. 2019, Revised: 27 Apr. 2019, Accepted: 3 May 2019

Published online: 1 Sep. 2019

Abstract: Computational techniques based on ranks of Hankel matrices (H -ranks) is used to study the convergence to Arnold tongues in the circle map. It appears that the process of convergence to the phase-locked mode of the discrete stationary attractor is far from being trivial. Figures of pseudoranks of Hankel matrices constructed from transient solutions of the circle map carry important physical information about complex nonlinear processes and are also beautiful from the aesthetical point of view.

Keywords: Hankel matrix; Circle map; Complexity of computation

1 Introduction

Clocking convergence is an important tool for investigating various aspects of iterative nonlinear maps. The rate of convergence to the critical attractor when an ensemble of initial conditions is uniformly spread over the entire phase space providing the insight into the fractal nature and the scale invariance of the dynamical attractor [1,2]. Numerical convergence of the discrete logistic map gauged with a finite computational accuracy is investigated in [3] where forward iterations are used to identify self-similar patterns in the region before the onset to chaos. An alternative technique based on the concept of the H -rank is proposed in [4] for clocking the convergence of iterative chaotic maps.

The main objective of this paper is to show that the concept of the H -rank can be effectively used for the investigation of convergence properties of the circle map. The insight into the embedded algebraic complexity of the nonlinear system is revealed by computing and visualizing of Hankel ranks in the space of system's parameters and initial conditions. It is shown in [4] that the computation of Hankel ranks can be effectively used to identify and assess the sensitivity of nonlinear systems to initial conditions and can be used as a simple and effective numerical tool for qualitative investigation of the onset of chaos for discrete nonlinear iterative maps.

We use the discrete iterative circle map to illustrate the process of convergence to stationary states. The circle

map is a paradigmatic model of a nonlinear iterative dynamical system used to study the dynamical behavior of a beating heart [5]. We show that the study of the convergence rate to a periodic orbit of the circle map can produce beautiful and appealing patterns. Moreover, these graphical pictures contain important information on the stability of periodic orbits of the circle map. This information could be useful whenever the manipulation or control of quasiperiodic nonlinear systems would be considered [6,7].

We also discuss the peculiarities of computer arithmetic in computations we perform. Floating point standard was explored in order to explain the fact of successful calculations down below the limit of machine epsilon.

2 The algorithm for the computation of the H -rank

The concept of the H -rank of a sequence $(p_j; j = 0, 1, \dots); p_j \in \mathbb{R}$; has been introduced in [4]. The purpose of this section is to recall the concept of the H -rank of a solution of a discrete iterative map. Corresponding sequence of Hankel matrices reads:

$$H_n := (p_{i+j-2})_{1 \leq i, j \leq n} =$$

* Corresponding author e-mail: mantas.landauskas@ktu.lt

$$= \begin{bmatrix} p_0 & p_1 & \cdots & p_{n-1} \\ p_1 & p_2 & \cdots & p_n \\ \cdots & \cdots & \cdots & \cdots \\ p_{n-1} & p_n & \cdots & p_{2n-2} \end{bmatrix}; n = 1, 2, \dots$$

The Hankel transform (the sequence of determinants of Hankel matrices) ($d_n; n = 0, 1, \dots$) reads:

$$d_n := \det H_n; n = 1, 2, \dots$$

Definition The sequence ($p_j; j = 0, 1, \dots$) has an H-rank $m \in \mathbb{Z}_0; m < +\infty$;

$$Hr(p_j; j = 0, 1, \dots) = m;$$

if the sequence of determinants of Hankel matrices has the following structure:

$$(d_1, d_2, \dots, d_m, 0, 0, \dots)$$

where $d_m \neq 0$ and $d_{m+1} = d_{m+2} = \dots = 0$.

It is admitted that $Hr(0, 0, 0, \dots) = 0$. Note that $Hr(p_0, \dots, p_m, 0, 0, 0, \dots) = m + 1$, if only $p_m \neq 0$ for $m = 0, 1, 2, \dots$

3 Floating point number arithmetic

All real numbers are stored as a closest binary number [8]:

$$x = (-1)^s \cdot (1 + Fraction) \cdot 2^{Exp-Bias}.$$

A floating point number of a double word length has the sign bit, 11 bits for Exp part and 52 bit for the fraction (or the mantissa) in 32bit system. The bias is set to 1023 thus largest power of 2 is $\sum_{i=0}^{10} 2^i - 1023 = 2^{11} - 1 - 1023 = 1024$ and the smallest power of 2 is $0 - 1023 = -1023$. The least significant bit is equal to $2^{-52} \approx 2.22 \cdot 10^{-16}$ (the machine epsilon). In this case the 16-th digit of the mantissa of a real number is approximate.

Consider the number $x = 3.5$. Mantissa must start with 1 so $\frac{x}{2^1} = 1.75$ gives $Exp - Bias = 1$ and 0.75 as fraction. $0.75 = \frac{1}{2} + \frac{1}{2^2} + \frac{0}{2^3} + \dots$. The number is positive, so $s = 0$ and we have these bits in computer memory (double format in a 32bit system): 01000...011000...0.

An important fact must be mentioned here. Consider two floating point numbers which differ less than machine epsilon (for example 2^{-21} and 2^{-20}). The arithmetic operations of course can be performed. Despite this one must be careful while working with detection of convergence or similar problems. The number might converge and become constant (if we fix the machine epsilon as being equivalent to zero) in computer memory but the difference between two adjacent numbers might still exist and might be less than machine epsilon. Thus there are problems where certain properties of computer arithmetic are important.

4 Notes on finding H-rank using floating point arithmetic

Suppose we have a sequence of numbers: 2.5; -1; 0.25; -0.06; -0.25; 0.1; 0.25; 0.1. Let these numbers be the orbit of a particular map of interest. Corresponding sequence of Hankel matrices is:

$$H^{(1)} = [2.5]; H^{(2)} = \begin{bmatrix} 2.5 & -1 \\ -1 & 0.25 \end{bmatrix};$$

$$H^{(3)} = \begin{bmatrix} 2.5 & -1 & 0.25 \\ -1 & 0.25 & -0.06 \\ 0.25 & -0.06 & -0.25 \end{bmatrix};$$

$$H^{(4)} = \begin{bmatrix} 2.5 & -1 & 0.25 & -0.06 \\ -1 & 0.25 & -0.06 & -0.25 \\ 0.25 & -0.06 & -0.25 & 0.1 \\ -0.06 & -0.25 & 0.1 & 0.25 \end{bmatrix}.$$

Firstly we have used MATLAB to find the determinants for each of the matrices above. Calculations resulted in: $d^{(1)} = 2.5$; $d^{(2)} = -0.375$; $d^{(3)} = 0.099125$; $d^{(4)} = 0.07683046$. Usually the results can be considered of acceptable accuracy because the number represented by the least significant bit in double format ($2^{-52} \approx 2.22 \cdot 10^{-16}$) is much less than the last digits of the results obtained.

The floating point arithmetic is simulated by writing a C++ code for performing “+”; “-”; “*” operations and calculating the determinant of a matrix by performing the product of first row elements and corresponding lower order determinants. The purpose of this is to see where accuracy is lost and, more importantly, to find out whether that correlates to the properties of the map.

Completely for the illustrative purposes custom floating point type is chosen here. 1 bit is dedicated to the sign of a number, 5 bits for the exponent and 6 bits for the mantissa. Setting 5 bits for the exponent enables one to use $2^{\pm(31-1)/2} = 2^{\pm 15} = \pm 32768$ as a maximal factor (because $2^0 + 2^1 + \dots + 2^4 = 31$). Analogously one can find the limits for a mantissa.

In this example $d^{(3)}$ is calculated as follows:

$$\begin{aligned} & 2.5 \cdot (0.25 \cdot (-0.25) - 0.06 \cdot 0.06) - \\ & - (-1) \cdot (-1 \cdot (-0.25) - (-0.06) \cdot 0.25) + \\ & + 0.25 \cdot (-1 \cdot (-0.06) - 0.25 \cdot 0.25). \end{aligned}$$

Some operations do not affect the accuracy of the result such as:

$0.25_{10} \times$	1.000000	$\cdot 2^{-2}$
0.25_{10}	1.000000	$\cdot 2^{-2}$
0.0625_{10}	1.000000	$\cdot 2^{-4}$

But some operations results in:

$0.06_{10} \times$	1.111000	$\cdot 2^{-5}$
0.06_{10}	1.111000	$\cdot 2^{-5}$
0.0035095_{10}	1.1100101	$\cdot 2^{-9}$

In this case the resulting number has a longer mantissa than 6 positions. The remaining bit $2^{-7} \cdot 2^{-9} = 2^{-16}$ is not stored in the resulting number. Depending on the hardware used for the calculations, this remaining bit most probably will be lost. Such accuracy loss is a price for length of the mantissa being too short.

It is not difficult to notice that in a certain case the two added numbers can differ more than the length of a mantissa. By performing addition and normalizing the mantissas in the first place one of the operands becomes zero in the mantissa. Thus it is not acting in the operation and the result will be the greater number of the two. To sum up, the operation in fact lies beyond the machine epsilon and is successfully performed. In other words, operations are performed in the exponent. However the accuracy of the result is then lost.

A number of acceptable accuracy losses is fixed while performing calculation of H -ranks. $k = \frac{n!}{2}$ shows to be the most informative and universal value obtained experimentally (here n is the order of the determinant being calculated). Nevertheless, this number is approximately equal to half of arithmetic operations in calculating determinant by expanding it to the sum of the product of one row elements and consecutive lower order determinants.

Suppose one needs to calculate the determinant by performing actions mentioned above. If determinant of order 2 is calculated as the difference of the products of the diagonal elements then 1 subtraction operation must be executed. The order 3 determinant requires 2 sums of cofactors and 3 · 1 subtractions inside each of them. The order 4 determinant requires 3 + 4 · 2 sums and 4 · 3 · 1 subtractions and so on. In this respect the order n determinant requires $(n - 1) + n \cdot ((n - 2) + (n - 1) \cdot ((n - 3) + (n - 2) \cdot \dots \cdot 3 \cdot 1))$ sums and $\frac{n!}{2}$ subtractions.

Order	Total sums of cofactors	Total subtractions of products	Total number of +-	$\frac{n!}{2}$
2	0	1	1	1
3	3 · 0 + 2 = 2	3	5	3.5
4	4 · 2 + 3 = 11	4 · 3 = 12	23	12
5	5 · 11 + 4 = 59	5 · 4 · 3 = 60	119	60

As seen from the table $\frac{n!}{2}$ is approximately half of the sum and subtraction operations present in finding the cofactor expansion for a particular determinant. The total number of these operations is $n! - 1$.

5 Visualization of the process of convergence to Arnold tongues

The circle map is represented by the one-dimensional iterative map:

$$\theta_{n+1} = f(\theta_n) = \theta_n + \Omega - \frac{K}{2\pi} \cdot \sin(2\pi\theta_n); \quad (1)$$

where θ_n value lies between 0 and 1 ($2\pi\theta_n$ is a polar angle); K is the coupling strength; Ω is the driving phase

and $n = 0, 1, \dots$ Figure 1 shows the bifurcation diagram for the circle map. The symmetry of the bifurcation diagram can suggest to perform a research in a subset of the domain of Ω . However this may not apply to the transients and it is important in clocking convergence.

The circle map exhibits a phenomenon called phase locking if small to intermediate values of K ($0 < K < 1$) and certain values of Ω are considered. In a phase-locked region, the values θ_n advance as a rational multiple of n . The phase-locked regions in $\Omega - K$ parameter plane are called Arnold tongues [9].

The H -rank is used as the computational tool for the reconstruction of Arnold tongues. At first H -ranks are computed in the region $0 \leq \Omega \leq 1$ and $0 \leq K \leq \pi$. For every pair of Ω and K the iterative process is started and the sequence $\{\theta_j\}; j = 0, 1, \dots$; is constructed; the initial condition θ_0 is set to 0.5; and calculate the H -rank of that sequence. As shown in [4], the H -rank of a chaotic sequence does not exist (the H -rank tends to infinity then). Therefore the upper limit for the H -rank $\bar{m} = 30$ is fixed. If the sequence of determinants does not vanish until $m = 30$ the process is terminated assuming that $Hr\{p_j\} = \bar{m}; j = 0, 1, \dots$. The results are shown in Figure 2(f). The more elements of the sequence $(\theta_j; j = 0, 1, \dots)$; are considered (leading to possible higher H -ranks of the sequence) the more resulting picture is alike to the well-known shape of Arnold tongues in the circle map [10].

6 The computation of pseudoranks

In order to determine the rank of the sequence one needs to find such matrix dimension $(\bar{m} + 1)$ that the determinant of the Hankel matrix is equal to zero. In practice it is sufficient to compute determinants up to a certain precision ϵ , like the machine epsilon. Calculating a determinant of a square real matrix requires a fair amount of computer resources if the dimension of a matrix is large. Moreover, the determinant, though being a conventional notion theoretically, rarely finds a useful role in numerical algorithms [11].

Plotting phase diagrams of H -ranks requires massive computations of determinants of Hankel matrices. Thus, instead of using a standard straightforward function *det* in MATLAB here C++ and the LAPACK package are employed to perform the computation of determinants of Hankel matrices. And though LAPACK can be considered as the state-of-the-art in linear algebra, it does not have a standard subroutine for the computation of the determinant. Instead, the standard PLU decomposition of a matrix into the lower triangular matrix L (having ones on the main diagonal), the upper triangular matrix U and the permutation matrix P is performed. The absolute value of the determinant of the original matrix is equal to the product of elements on the main diagonal of U . The number of permutations determines the sign of the determinant of the original matrix. But since the absolute

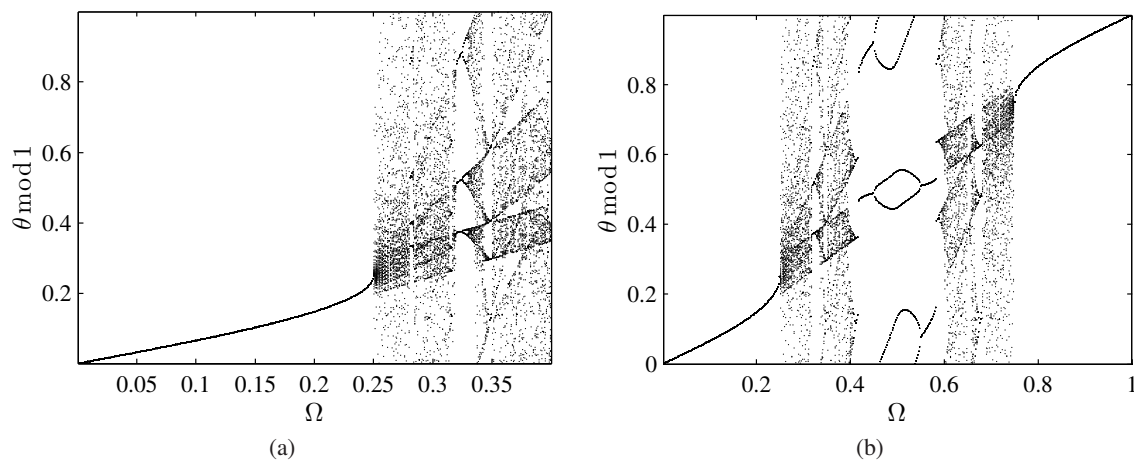


Fig. 1: The bifurcation diagram for the circle map at $K = \frac{\pi}{2}$. The first 10000 orbit points are omitted.

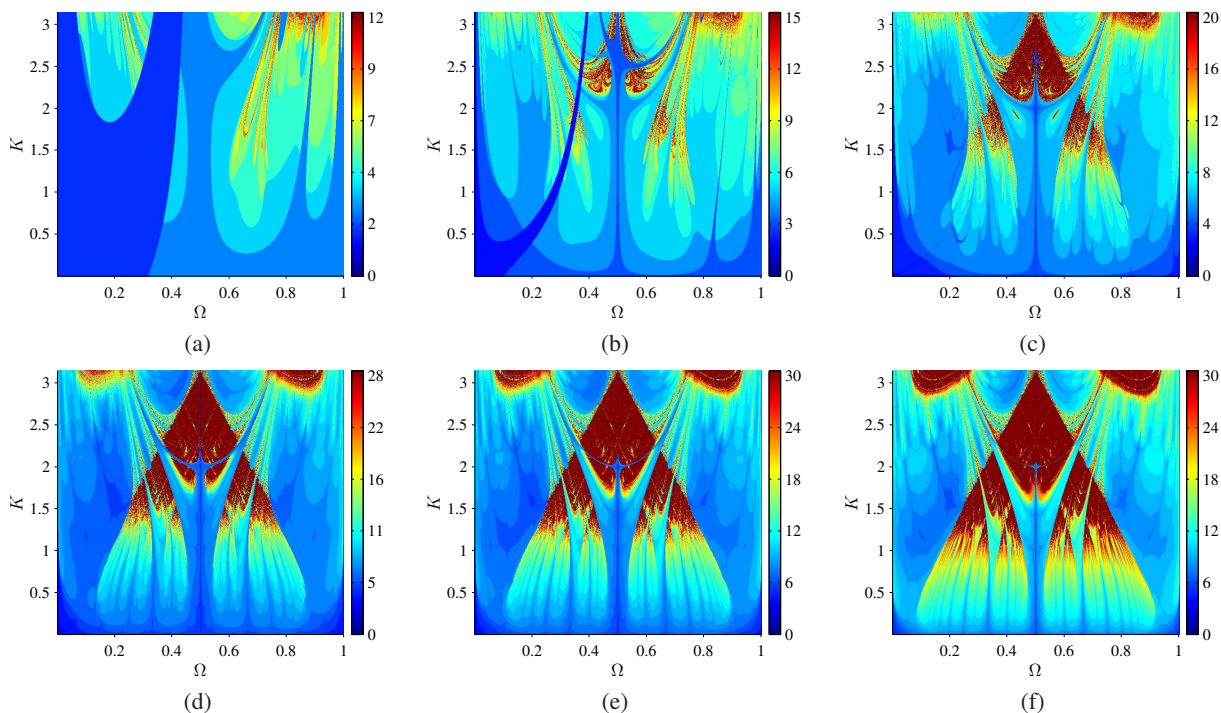


Fig. 2: Maps of pseudoranks for different initial conditions ($0 \leq \Omega \leq 1$, $0 \leq K \leq \pi$ and $\theta_0 = 0.5$) at (a): $\varepsilon = 10^{-1}$; (b): $\varepsilon = 10^{-2}$; (c): $\varepsilon = 10^{-4}$; (d): $\varepsilon = 10^{-8}$; (e): $\varepsilon = 10^{-12}$; (f): $\varepsilon = 10^{-20}$.

value of the determinant is of interest only, it suffices to compute the product of diagonal elements of U . An alternative approach could be counting the number of non-zero diagonal elements. The computation of determinants is continued as the product of diagonal elements of the matrix U until $|\det H_{m+1}| < \varepsilon$. In this respect our computations reveal not the rank, but the pseudorank of a sequence.

The combination of the speed of C++ in performing loops (opposite to MATLAB) and the mathematical precision of LAPACK resulted in significantly faster formation of images of H -ranks in various phase planes. It can be noted that final visualization is performed using the functionality of MATLAB graphical functions.

The selection of a particular value of ε requires additional attention. As mentioned previously, the structure of Arnold tongues in the circle map is

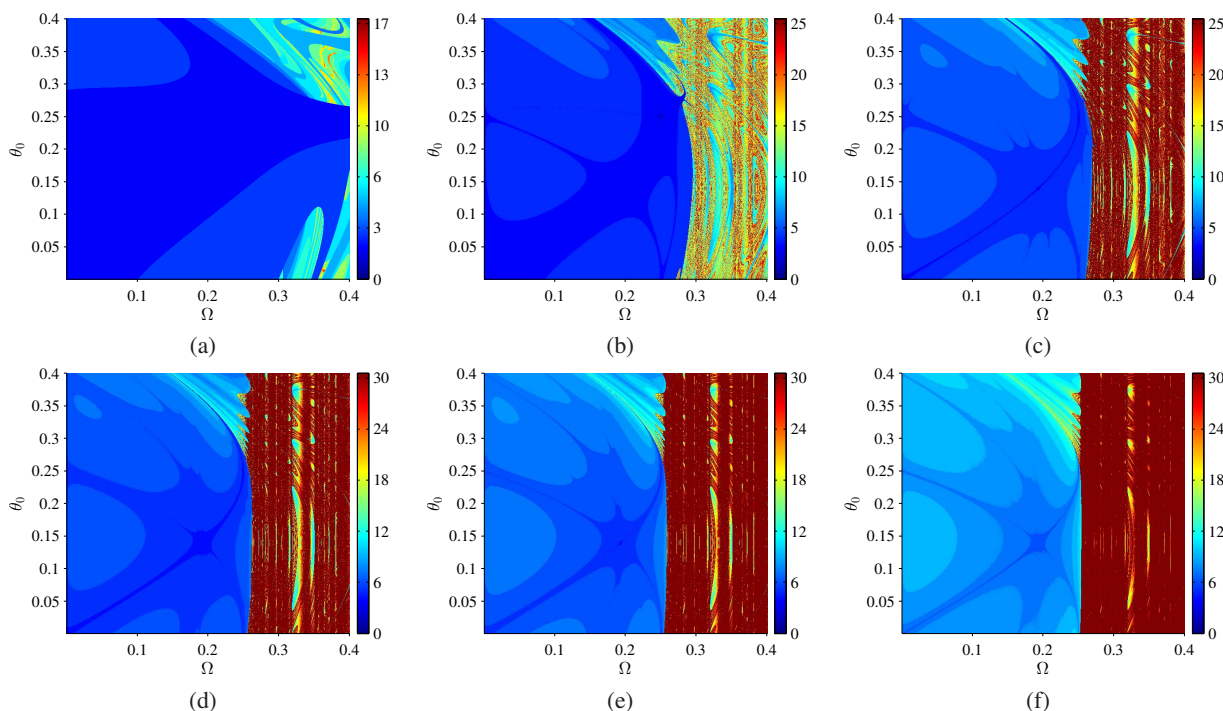


Fig. 3: Maps of pseudoranks for different initial conditions ($0 \leq \Omega \leq 0.4, 0 \leq \theta_0 \leq 0.4$ and $K = \frac{\pi}{2}$) at (a): $\varepsilon = 10^{-2}$; (b): $\varepsilon = 10^{-5}$; (c): $\varepsilon = 10^{-10}$; (d): $\varepsilon = 10^{-16}$; (e): $\varepsilon = 10^{-25}$; (f): $\varepsilon = 10^{-50}$.

well-known. The computation of pseudoranks for different initial conditions ($0 \leq \Omega \leq 1, 0 \leq K \leq \pi$ and $\theta_0 = 0.5$) for different ε is performed. Results are illustrated in Figure 2. The evolution of interesting patterns of pseudoranks can be observed as the value of ε is decreased (note that the maximum rank in colorbars is detected automatically and depends on ε).

A naked eye cannot see principal differences between Figure 2(e) and Figure 2(f). At this point one can fix the value of ε and use it for the construction of maps of pseudoranks. But the particular selection must be valid. In order to achieve this the graph representing the absolute root mean square difference E between consecutive maps of pseudoranks in Figure 2 is constructed. Let us denote $Hr_1(i, j)$ the value of the pseudorank at the i -th row and the j -th column of the map of pseudoranks computed at ε_1 (analogously $Hr_2(i, j)$ is the pseudorank at ε_2). Then, the difference E is defined as:

$$E(\varepsilon_2) = \sqrt{\frac{1}{mn} \sum_{i=1}^n \sum_{j=1}^m (Hr_1(i, j) - Hr_2(i, j))^2}$$

where m is the number of rows and n is the number of columns in maps of pseudoranks. The relationship $E(\varepsilon)$ is shown in Figure 4. It can be clearly seen that maps of pseudoranks do not change considerably beyond $\varepsilon = 10^{-25}$ and the limit of accuracy of double floating point arithmetic is reached.

The graph representing E between consecutive maps of pseudoranks on the subset of the parameter plane $\Omega - K$ at $[0; 0.4] \times [0; 0.5\pi]$ (Figure 2) is also constructed. In this case the detail of parameter plane improves more after the limit of accuracy of double floating point arithmetic.

7 The quality of the parameter planes near the manifolds of convergence

A comparison between Figure 4 and Figure 5 shows that distribution of accuracy of computations may not be uniform over the parameter plane. One of the essential elements of particular parameter plane are stable and unstable manifolds. Vicinities of these manifolds contain orbits of different dynamical qualities. These differences can also be explained as being different in complexity which in turn has effect on the accuracy of the computations.

Such heuristic argument is explored further by constructing the manifolds of convergence for the circle map and comparing them to the plots of accuracy loss detection of pseudorank calculations. The plot of accuracy loss detection in Figure 7(b) shows the minimal order of the determinant calculated with at least $\frac{n!}{2}$ accuracy losses in arithmetical operations.

To construct stable and unstable manifolds one needs to find fixed points of the map. By solving $f(\theta) = \theta$

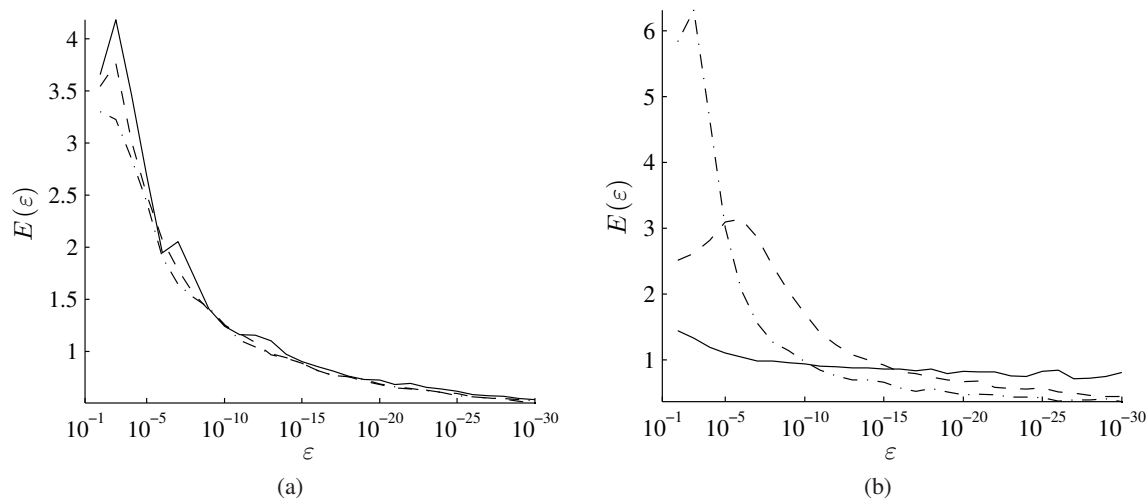


Fig. 4: The relationship between the absolute root mean square difference E and the ε at $m = 30$. Calculations are performed using parameter plane $\Omega - K$ of dimensions $[0; 1] \times [0; \pi]$ (a) (the solid line represents the variation of E at $\theta_0 = 0.25$; the dashed line - at $\theta_0 = 0.5$; the dotted and dashed line - at $\theta_0 = 0.75$) and $\Omega - \theta_0$ of dimensions $[0; 1] \times [0; 1]$ (b) (the solid line represents the variation of E at $K = 0.25\pi$; the dashed line - at $K = 0.5\pi$; the dotted and dashed line - at $K = 0.75\pi$).

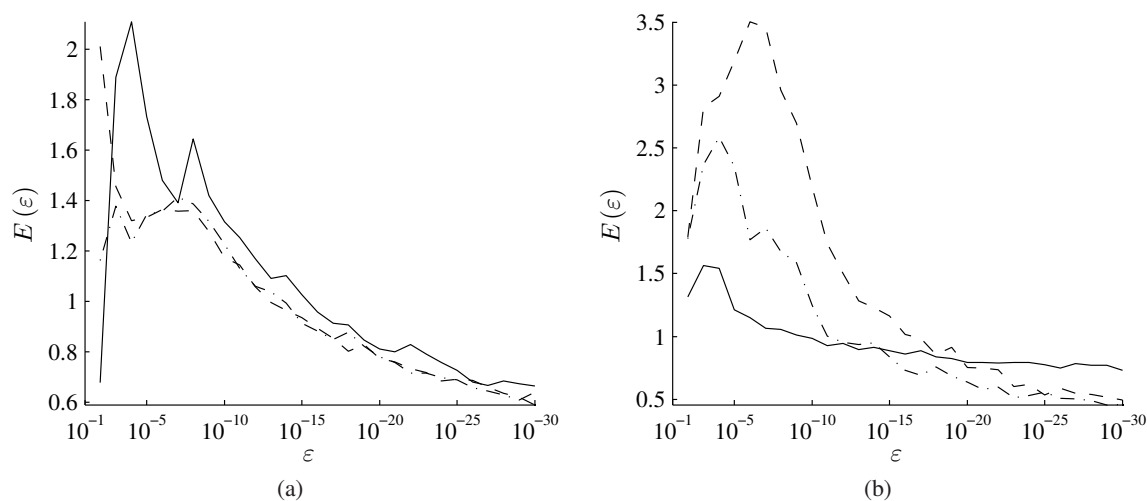


Fig. 5: The relationship between the absolute root mean square difference E and the ε at $m = 30$. Calculations are performed using parameter plane $\Omega - K$ of dimensions $[0; 0.4] \times [0; 0.5\pi]$ (a) (the solid line represents the variation of E at $\theta_0 = 0.25$; the dashed line - at $\theta_0 = 0.5$; the dotted and dashed line - at $\theta_0 = 0.75$) and $\Omega - \theta_0$ of dimensions $[0; 0.4] \times [0; 0.4]$ (b) (the solid line represents the variation of E at $K = 0.25\pi$; the dashed line - at $K = 0.5\pi$; the dotted and dashed line - at $K = 0.75\pi$).

fixed points $\theta = \frac{(-1)^k \arcsin \frac{2\pi\Omega}{K} + \pi k}{2\pi}$, $k \in \mathbb{Z}$, are obtained. Previous computations were performed on the domain $[0; 1] \times [0; 1]$ (or a subset of it) in the plane $\Omega - K$. Thus $k = 0$ is fixed and the following equations for stable and unstable manifolds are obtained.

$$\theta = \begin{cases} \frac{\arcsin \frac{2\pi\Omega}{K}}{2\pi}, \\ \frac{\pi - \arcsin \frac{2\pi\Omega}{K}}{2\pi}. \end{cases}$$

Figure 6 shows the comparison of constructed manifolds to the manifold of non-asymptotic convergence.

If the manifold of non-asymptotic convergence is compared to the plot of accuracy losses (Figure 7(b)) some interesting similarities are seen. A part of the manifold corresponds to the initial conditions leading to fewer accuracy losses were mentioned before. This fact suggests that one must pay more attention to the various manifolds whenever the quality and detail of parameter

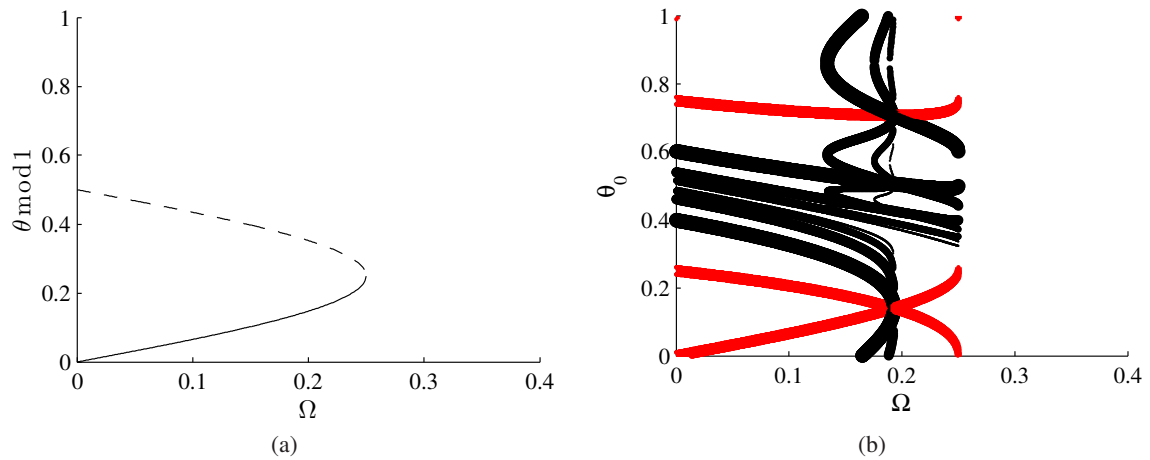


Fig. 6: (a) The stable (solid line) and the unstable (dashed line) manifolds for the circle map at $K = \frac{\pi}{2}$. (b) The manifold of non-asymptotic convergence to period-1 regime at $K = \frac{\pi}{2}$. The thickness of black solid lines illustrates the number of forward iterations required to reach the period-1 regime; the red solid line stands for period-1 regimes.

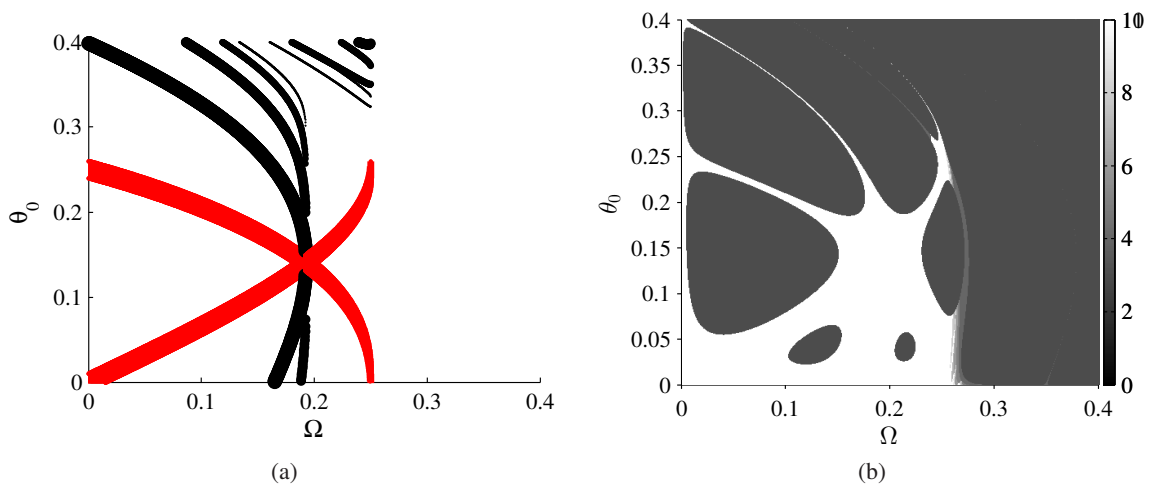


Fig. 7: The comparison of the manifold of non-asymptotic convergence (to period-1 regime) to the plot of accuracy loss detection ($\epsilon = 10^{-16}$, $K = \frac{\pi}{2}$, $k = \frac{n!}{2}$).

planes is considered. The other areas of the parameter plane corresponds to the most accuracy losses. A logical explanation for this result might be the heuristic argument mentioned before. An orbit which is relatively far from the manifold of convergence tend to act more chaotic. This in turn leads to higher order determinants being considered.

8 Concluding remarks

The existence of Arnold tongues in the circle map is known for already more than five decades ago [12]. There exist different computational techniques for the visualization of Arnold tongues. The universal algorithm

for the identification of Arnold tongues is based on two simple steps. At first, the system must be iterated far away from initial conditions until all transient processes cease down. Secondly, one must identify the effect of the phase locking in the discrete stationary attractor. Different modes of the phase locking are then visualized by different colors.

The method discussed also consists of two steps and can be used for visualizing Arnold tongues themselves. Firstly the system is iterated for a predetermined number of steps from initial conditions. Then one does not need to search for the effect of the phase locking. Then simple computation of the H -rank of the stationary signal is performed and Arnold tongues occur in the phase plot of

pseudoranks. Thus the quality of phase diagrams is crucial whenever the manipulation or control of quasiperiodic nonlinear systems would be considered.

A much more interesting question is about the convergence properties of the circle map to Arnold tongues. It has been shown previously that pseudoranks of transient processes may reveal important physical information about the properties of a discrete system. For example, it has been shown in [9] that one can observe the stable, the unstable manifold and the manifold of nonasymptotic convergence in the plotted phase diagrams of the logistic map. In this paper the H -rank of the transient processes of the circle map has been used for the visualization of the rate of convergence to the Arnold tongues. Optimal selection of the value for ε has been considered.

Acknowledgement

Financial support from the Lithuanian Science Council under project No. MIP-078/2015 is acknowledged.

References

- [1] F. A. B. F. de Moura, U. Tirnakli, M. L. Lyra, Convergence to the critical attractor of dissipative maps: long-periodic oscillations, fractality, and nonextensivity, *Physical Review E*, **62**, 6361-6365 (2000).
- [2] R. Tonelli, M. Coraddu, Numerical study of the oscillatory convergence to the attractor at the edge of chaos, *The European Physical Journal B*, **50**, 355-359 (2006).
- [3] C. L. Bresten, Jung Jae-Hun, A study on the numerical convergence of the discrete logistic map, *Commun Nonlinear Sci Numer Simul*, **14**, 3076-3088 (2009).
- [4] M. Ragulskis, Z. Navickas, The rank of a sequence as an indicator of chaos in discrete nonlinear dynamical systems, *Commun Nonlinear Sci Numer Simul*, **16**, 2894-2906 (2011).
- [5] L. Glass, M. R. Guevara, A. Shrier, R. Perez, Bifurcation and Chaos in a Periodically Stimulated Cardiac Oscillator, *Physica 7D*, **7**, 89-101 (1983).
- [6] M. Landauskas, J. Ragulskienė and M. Ragulskis, H -rank as a control tool for discrete dynamical systems, in AIP Conference Proceedings, **1479**, 2098-2101, (2012).
- [7] M. Landauskas and M. Ragulskis, Clocking convergence to Arnold tongues - the H -rank approach, in AIP Conference Proceedings, **1558**, 2457-2460, (2013).
- [8] IEEE Standard for Binary Floating-Point Arithmetic, *Computer Magazine*, **14**, (1981).
- [9] P. L. Boyland, Bifurcations of circle maps: Arnold tongues, bistability and rotation intervals, *Communications in Mathematical Physics*, **106**, 353-381 (1986).
- [10] F. Schilder, B. B. Peckham, Computing Arnold tongue scenarios, *Journal of Computational Physics*, **220**, 932-951 (2007).
- [11] L. N. Trefethen, *Numerical linear algebra*, SIAM, (1997).
- [12] V. I. Arnold, Small denominators. I: On the maps of a circle onto itself, *Izv. Akad. Nauk SSSR Ser. Mat.*, **25**, 21-86 (1961).



Mantas Landauskas received the PhD degree in informatics in 2016 from the Kaunas University of Technology, Lithuania. He is currently a lecturer in Department of mathematical modelling, Kaunas University of Technology. His research is mostly about creating the methodology for clocking convergence and controlling of nonlinear dynamical systems (discrete or continuous) using computational techniques based on ranks of Hankel matrices (H-ranks).



Minvydas Ragulskis received the Ph.D. degree in 1992 from Kaunas University of Technology, Lithuania. Since 2002 he is a professor at the Department of Mathematical modelling, Kaunas University of Technology. His research interests include nonlinear dynamical systems and numerical analysis. He is the founder and head of the Center for Nonlinear Systems (<http://www.personalas.ktu.lt/~mragul>).